*Research Article*

# A Comparison of the Mechanical Properties of the Goat Temporomandibular Joint Disc to the Mandibular Condylar Cartilage in Unconfined Compression

**Catherine K. Hagandora, Thomas W. Chase, and Alejandro J. Almarza**

*Department of Oral Biology, Department of Bioengineering, Center for Craniofacial Regeneration,*
*McGowan Institute of Regenerative Medicine, University of Pittsburgh, Pittsburgh, PA, 15261, USA*

Correspondence should be addressed to Alejandro J. Almarza, aja19@pitt.edu

The aim of this study was to make a comparison of the compressive properties of the goat temporomandibular joint (TMJ) disc to the mandibular condylar cartilage (MCC) and to explore the transversely isotropic biphasic model. Samples taken mediolaterally from three regions of the TMJ disc and MCC were tested in unconfined compression at strain levels ranging from 10% to 50% and then assessed for biochemical content. The results indicated that the TMJ disc exhibits a significantly greater tangent modulus than the MCC from 20% to 50% strain with values ranging from $729 \pm 267$ to $2413 \pm 406$ kPa and $363 \pm 169$ to $1677 \pm 538$ kPa, respectively ($P < .05$). The collagen content of the TMJ disc was significantly greater than the MCC, while the opposite held for the glycosaminoglycan (GAG) and DNA content. The results emphasize fundamental differences between the articulating tissues of the TMJ.

## 1. Introduction

The temporomandibular joint (TMJ) is a synovial, bilateral joint formed by the articulation of the condyle of the mandible and the articular eminence and glenoid fossa of the temporal bone. It is estimated that 10 million Americans are affected by TMJ disorders (TMDs), a term encompassing a variety of conditions which result in positional or structural abnormalities in the joint [1]. Indications of TMDs can include pain, clicking, locking, headaches, joint pain/tenderness, restricted range of motion, and painful mastication [2]. While in many instances the cause is unknown, 11% of individuals with TMJ disorders have symptoms of TMJ osteoarthrosis [3], a pathology which can lead to a cascade of problems resulting from functional and morphological changes in the joint [4]. Additionally, up to 70% of people with TMJ disorders suffer from displacement of the TMJ disc or "internal derangement" of the TMJ [5]. Due to the frequency and severity of these conditions, it is necessary to formulate a more comprehensive understanding of the role of healthy articulating tissues in TMJ function.

The primary function of the TMJ is to facilitate mandibular motion. The fossa remains stationary throughout jaw movement, while the mobile portions of the joint include the condyles of the mandible. A fibrocartilage disc is positioned between the inferior surface of the articular eminence and the superior surface of the mandibular condyle. The TMJ disc helps joint motion by distributing compressive, tensile, and shear forces [6]. The TMJ disc has a biconcave geometry and the primary extracellular matrix (ECM) components of the disc are collagen, proteoglycans, and elastic fibers. The mandibular condyles consist of bone with a fibrocartilage layer on the articulating surface. The mandibular condylar cartilage (MCC) is considerably thinner than the TMJ disc [7–12], lies adjacent to subchondral bone, and possesses a distinct zonal organization.

Characterization of the properties of the articulating tissues of the joint is a necessary prequel to understanding the process of pathogenesis as well as tissue-engineering suitable constructs for replacement of damaged joint fibrocartilage. In tissue-engineering approaches for fibrocartilage, goat costal chondrocytes have proven to be a viable cell source

for scaffoldless tissue-engineering constructs, due to their production of high quantities of collagen and GAG [13, 14]. These studies show the potential for the goat as a tissue engineering model. However, a comprehensive mechanical characterization has not been performed. Furthermore, the current literature lacks a one-to-one comparison of the regional compressive behavior of the goat MCC to the TMJ disc. Since these tissues work synchronously during mandibular movement, a comparison of their properties is necessary to provide insight into how the articulating surfaces of the joint work as a unit.

To date, a phenomenological model has not been utilized to describe the unconfined compressive behavior of the goat TMJ tissues. The TMJ disc and MCC in other species have been characterized as highly organized hydrated, porous, and permeable solid extracellular matrix tissues [15–17]. The biphasic theory has been shown to successfully model the behavior of articular cartilage, a similar tissue to the disc and MCC, by applying two distinct fluid and solid phases [18]. However, it is known that the fibers of the TMJ disc run anteroposteriorly in the medial, lateral, and intermediate zones [19]. Furthermore, the most superior zone of the MCC has also been shown to possess a transverse collagen arrangement [20]. Taking into account this fiber alignment, the transversely isotropic biphasic model may provide an accurate account for the mechanical behavior of TMJ fibrocartilage when exposed to compressive forces [21].

The aim of this study was to characterize and compare the intermediate zone, medial, and lateral regions of the goat TMJ disc and MCC under unconfined compression. A simple mechanical analysis was used to calculate the percent relaxation and tangent modulus of the various tissue regions. Additionally, curve fitting the experimental data to the transversely isotropic biphasic model allowed for determination of transverse and axial Young's moduli, transverse and axial Poisson's ratios, and tissue permeability. Additionally, biochemical analysis was performed to determine the comparative collagen, GAG, and DNA content of the various regions. We hypothesized that the transversely isotropic biphasic model can be used to describe the stress relaxation behavior of both the TMJ disc and MCC in unconfined compression. The results will provide for a more comprehensive understanding of the mechanical behavior of the articulating tissues of the TMJ.

## 2. Methods

### 2.1. Mechanical Testing.
Eight skeletally mature Boer goat heads were obtained from a local abattoir and dissected to isolate the disc and MCC within 24 hours of death. A 4 mm circular biopsy punch was used to obtain the medial, lateral, and intermediate sections from the disc and condylar cartilage (Figure 1). Specimens were wrapped in gauze, wetted in phosphate buffered saline (PBS), and stored at −20°C until testing. This method of storage was utilized, because it has previously been shown to have no effect on the material properties of the porcine TMJ disc [22]. Prior to testing, samples were allowed to equilibrate for 1

hour in PBS. The tissue punches were then attached to a compression platen using cyanoacrylate with the inferior surface of the disc and the superior surface of the condyle facing up. The specimen diameter was measured prior to testing using digital calipers. To estimate specimen height, force was applied to the sample until reaching 0.05 N, at which point the crosshead position was noted and the platen was immediately removed. The water bath was then filled with PBS and the thermocouple was set to 37°C prior to testing. The MTS Insight was used to measure changes in force throughout the test. The upper platen was lowered within 0.1 mm of the determined specimen height and a preload of 0.05 N was applied for 30 min. The height at the end of the preload was taken to be the height of the specimen and was utilized in subsequent calculations. The specimens then underwent 10 cycles of preconditioning at 9%/min until 10% strain was reached. The strain rate parameter was determined by Sergerie et al. for applying the transversely isotropic biphasic model to cartilage [23]. Immediately following preconditioning, a series of five stress relaxation tests were performed. The samples were compressed in 10% increments until 50% strain was reached and were allowed to relax for thirty minutes between increments.

### 2.2. Compression Analysis.
A simple analysis was first used to evaluate the data. A tangent modulus was fit to the linear portion of the stress strain curve using Matlab. The linear portion was defined as the last 2% strain of the ramping phase of each 10% increment. The percent relaxation was determined by evaluating the ratio of the stress of the relaxed specimen, with the specimen considered fully relaxed at 30 min, to the peak stress.

The transversely isotropic biphasic model [21] was used to assess the mechanical properties of the three sections of the disc and condylar cartilage. The model allows for the determination of Young's moduli in the transverse and axial planes ($E_1$ and $E_3$), Poisson's ratios for the transverse and axial planes ($\nu_{21}$ and $\nu_{31}$), and the transverse permeability coefficient ($k$). As previously described [23], a four-parameter optimization procedure was performed to find $k$, $E_1$, $\nu_{21}$, and $\nu_{31}$. Briefly, the Young's modulus in the axial plane ($E_1$) was derived from the experimentally obtained relaxation stress. Using Matlab and the root mean square error method, the experimental data was fitted to analytical curves provided by the model. In (1)-(2), $\alpha_n$ are the roots of (7), where $J_0$ and $J_1$ are Bessel functions of the first kind, and the numbers of summations ($n$) used was the number of convergences to 0 for values of $x$ ranging from 0 to 20 (in increments of 0.01). The root equaling zero was programmed to be greater than −0.02 but less than 0.04. The constants $\Delta_1$, $\Delta_2$, $\Delta_3$, and $C_{11}$ (3)–(6) are calculated after (7) [21]. These constants were then used to determine the loading force (1) and relaxation force (2).

The uniqueness of the curve fits was tested using several sets of initial values. 81 different combinations of initial values were used to perform the fit, utilizing 3 guesses for each parameter. The initial guesses for each parameter ranged in equal increments from 0.1 to 0.5 for $\nu_{21}$ and $\nu_{31}$,
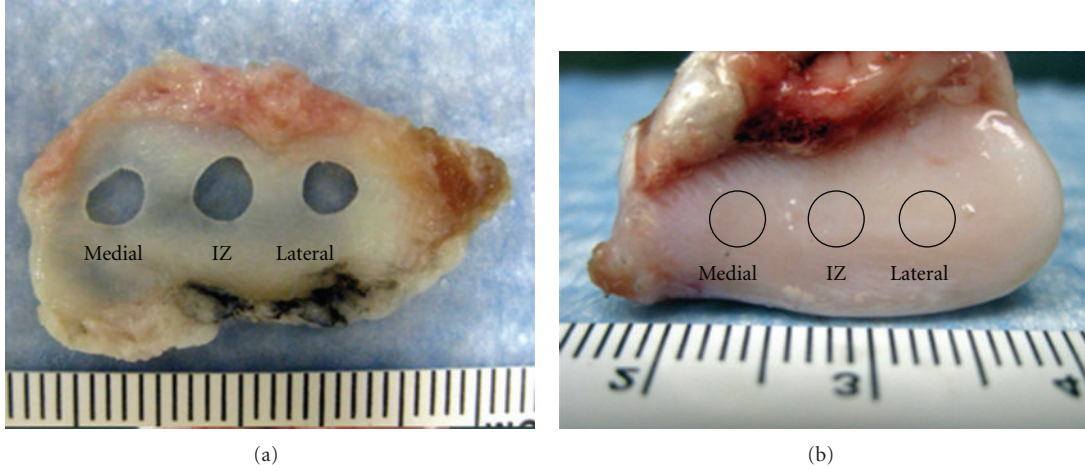
(a)



(b)

FIGURE 1: (a) TMJ disc and (b) MCC. The three test sites (medial, intermediate zone (IZ), and lateral) are indicated on each specimen.

0.1 MPa to 10 MPa for $E_1$, and $1 \times 10^{-14}$ m$^4$/Ns to $7 \times 10^{-14}$ m$^4$/Ns for $k$. The final parameters were the resulting average of all solutions with an error less than 1.5 times the minimum error found for all 81 guesses that complied with thermodynamic restrictions for a transversely isotropic material (8)-(9) [24]. The model was not fit to individual curves but the average curve of each tissue per strain step. The average force response, thickness, and radius of all sections of the TMJ disc and MCC were used to obtain a set of parameters for each strain level

$$f(t) = E_3 \dot{\epsilon}_0 t + E_1 \frac{\dot{\epsilon}_0 a^2}{C_{11} k} \Delta_3$$
$$\times \left[ \frac{1}{8} - \sum_{n=1}^{\infty} \left\{ \frac{\exp(-\alpha_n^2 C_{11}(kt/a^2))}{\alpha_n^2 [\Delta_2^2 \alpha_n^2 - (\Delta_1/(1+\nu_{21}))]} \right\} \right], \quad (1)$$
$$0 < t < t_0,$$

$$f(t)$$
$$= E_3 \dot{\epsilon}_0 t_0 - E_1 \frac{\dot{\epsilon}_0 a^2}{C_{11} k} \Delta_3$$
$$\times \sum_{n=1}^{\infty} \frac{\exp(-\alpha_n^2 C_{11}(kt/a^2)) - \exp[-(\alpha_n^2 C_{11} k(t-t_0))/a^2]}{\alpha_n^2 [\Delta_2^2 \alpha_n^2 - (\Delta_1/(1+\nu_{21}))]},$$
$$t > t_0, \quad (2)$$

$$\Delta_1 = 1 - \nu_{21} - 2\nu_{31} \left( \frac{E_1}{E_3} \right), \quad (3)$$

$$\Delta_2 = \frac{1 - \nu_{31}^2(E_1/E_3)}{1 + \nu_{21}}, \quad (4)$$

$$\Delta_3 = (1 - 2\nu_{31}^2) \frac{\Delta_2}{\Delta_1}, \quad (5)$$

$$C_{11} = \frac{E_1(1 - \nu_{31}^2)(E_1/E_3)}{(1 + \nu_{21})\Delta_1}, \quad (6)$$

$$J_1(x) - \left( \frac{1 - \nu_{31}^2(E_1/E_3)}{1 - \nu_{21} - 2\nu_{31}^2(E_1/E_3)} \right) x J_0(x) = 0, \quad (7)$$

$$\left( 1 - \nu_{31}^2 \frac{E_1}{E_3} \right), (1 - \nu_{21}^2) > 0, \quad (8)$$

$$1 - \nu_{21}^2 - \nu_{31}^2, \frac{E_1}{E_3} - 2\nu_{21}\nu_{31}^2 \frac{E_1}{E_3} > 0. \quad (9)$$

*2.3. Biochemistry.* The mechanically tested specimens were allowed to equilibrate for one hour in phosphate buffered saline, and the wet weights were measured. The specimens were lyophilized for 48 hours in order to obtain the dry weight. The samples were then digested in a papain solution, 125 $\mu$g/mL papain in 50 mmol phosphate buffer containing 5 mmol N-acetyl cystein overnight at 60°C [25]. The total hydroxyproline content of the tissue sections was assessed using the modified protocol of reacting the samples with chloramine T and dimethylaminobenzaldehyde that allows for a colorimetric comparison [26]. The samples were run against both hydroxyproline and collagen standards, and it was found that collagen is approximately 9% hydroxyproline. This value was used to calculate the collagen content of the samples. The DNA content was measured using a PicoGreen dsDNA Quantitation Kit (Molecular Probes, Inc., Eugene, Oregon). The total amount of glycosaminoglycan was measured using a dimethymethylene blue colorimetric assay kit (Biocolor; Newtownabbey, UK).

*2.4. Histology.* Histological analysis with polarized light microscopy was performed to visualize any damage to the collagen network from the high strains imposed. Samples from tested (right, intermediate zone) and untested (left, intermediate zone) goat TMJ discs were embedded in OCT freezing medium and flash frozen in −80°C. The samples were cryosectioned to 12 $\mu$m in the transverse and axial planes, stained with hematoxylin and eosin, and imaged using polarized light.

*2.5. Statistical Analysis.* A three-way ANOVA was used to assess differences between biomechanical values based on

TABLE 1: Peak stress, equilibrium stress, percent relaxation, and tangent modulus (mean ± standard deviation) of the TMJ disc and MCC (regions combined). Means within a column that do not share a letter have a difference that is statistically significant ($P < .05$).

| Tissue | Strain level | Peak stress (kPa) | Equilibrium stress (kPa) | % Relaxation | Tangent modulus (kPa) |
|---|---|---|---|---|---|
| TMJ disc | 10 | 16 ± 7<br>E | 2 ± 1<br>D | 85 ± 7<br>A | 304 ± 141<br>F |
|  | 20 | 61 ± 26<br>D | 6 ± 4<br>CD | 89 ± 7<br>A | 729 ± 267<br>D |
|  | 30 | 127 ± 40<br>C | 17 ± 12<br>CD | 87 ± 9<br>A | 1278 ± 385<br>C |
|  | 40 | 203 ± 48<br>B | 45 ± 33<br>BC | 79 ± 12<br>A | 1856 ± 429<br>B |
|  | 50 | 291 ± 63<br>A | 122 ± 75<br>A | 61 ± 17<br>B | 2413 ± 406<br>A |
| MCC | 10 | 11 ± 5<br>E | 2 ± 1<br>D | 85 ± 6<br>A | 205 ± 107<br>F |
|  | 20 | 35 ± 17<br>DE | 6 ± 4<br>CD | 84 ± 7<br>A | 363 ± 169<br>EF |
|  | 30 | 71 ± 30<br>D | 17 ± 11<br>BCD | 78 ± 10<br>A | 616 ± 237<br>DE |
|  | 40 | 132 ± 52<br>C | 56 ± 38<br>B | 62 ± 18<br>B | 1077 ± 359<br>C |
|  | 50 | 238 ± 94<br>B | 152 ± 92<br>A | 42 ± 23<br>C | 1677 ± 538<br>B |

TABLE 2: Average transverse Young's modulus ($E_1$), axial Young's modulus ($E_3$), transverse Poisson's ratio ($\nu_{21}$), axial Poisson's ratio ($\nu_{31}$), and tissue permeability ($k$) of the TMJ disc and MCC (regions combined).

| Tissue | Strain level | $E_1$ (MPa) | $E_3$ (MPa) | $\nu_{21}$ | $\nu_{31}$ | $k$ ($10^{-14}$ m$^4$/Ns) |
|---|---|---|---|---|---|---|
| TMJ disc | 10 | 0.18 | 0.02 | 0.10 | 0.02 | 4.47 |
|  | 20 | 0.97 | 0.07 | 0.23 | 0.05 | 0.78 |
|  | 30 | 1.93 | 0.17 | 0.17 | 0.06 | 0.31 |
| MCC | 10 | 0.14 | 0.01 | 0.10 | 0.00 | 5.48 |
|  | 20 | 0.61 | 0.06 | 0.21 | 0.02 | 1.70 |
|  | 30 | 1.22 | 0.17 | 0.23 | 0.03 | 0.90 |

tissue type, region, and strain level for the following factors: peak stress, equilibrium stress, tangent modulus, and percent relaxation. The model utilized can be described as follows: region ($A$) is nested within tissue (disc or MCC) ($B$) and both region and tissue are crossed with strain level ($C$) (10). To determine the differences between biochemical values a two-way ANOVA was used based on tissue type and region for the following factors: collagen content per dry weight, GAG content per dry weight, DNA content per dry weight, and percent water per wet weight. Tukey's post hoc testing was used to examine differences between groups for both analyses. All statistical analysis was performed using Minitab.

$$AB(A)CA * CB * C. \qquad (10)$$

## 3. Results

The results from the mechanical assessment showed no statistically significant differences between the three regions in both the MCC and TMJ disc for each strain level.

Therefore, the results are expressed in terms of tissue type (TMJ disc and MCC) for each strain level in Figures 2 and 3 and Tables 1 and 2.

*3.1. Simple Analysis.* The results from the simple compression analysis are shown in Figure 2 for a comparison between the disc and MCC and in Table 1 for a further comparison across strain step. The differences in peak stress (Figure 2(a)) between the two tissue types becomes more profound after 20% strain with the TMJ disc reaching a peak stress that is significantly higher than the MCC ($P < .05$). For example, at 30% strain, the disc reaches a peak stress of 127 ± 40 kPa which is significantly greater than the MCC at 71 ± 30 kPa ($P < .05$). There were also significant differences in peak stress between strain levels for both tissues (Table 1). For example, at 30% strain the peak stress of the disc is 127 ± 40 kPa which is significantly greater than the peak stress of 61 ± 26 kPa at 20% strain. For the MCC, at 40% strain the peak stress is 132 ± 52 kPa, which is significantly greater than the peak stress of 71 ± 30 kPa at
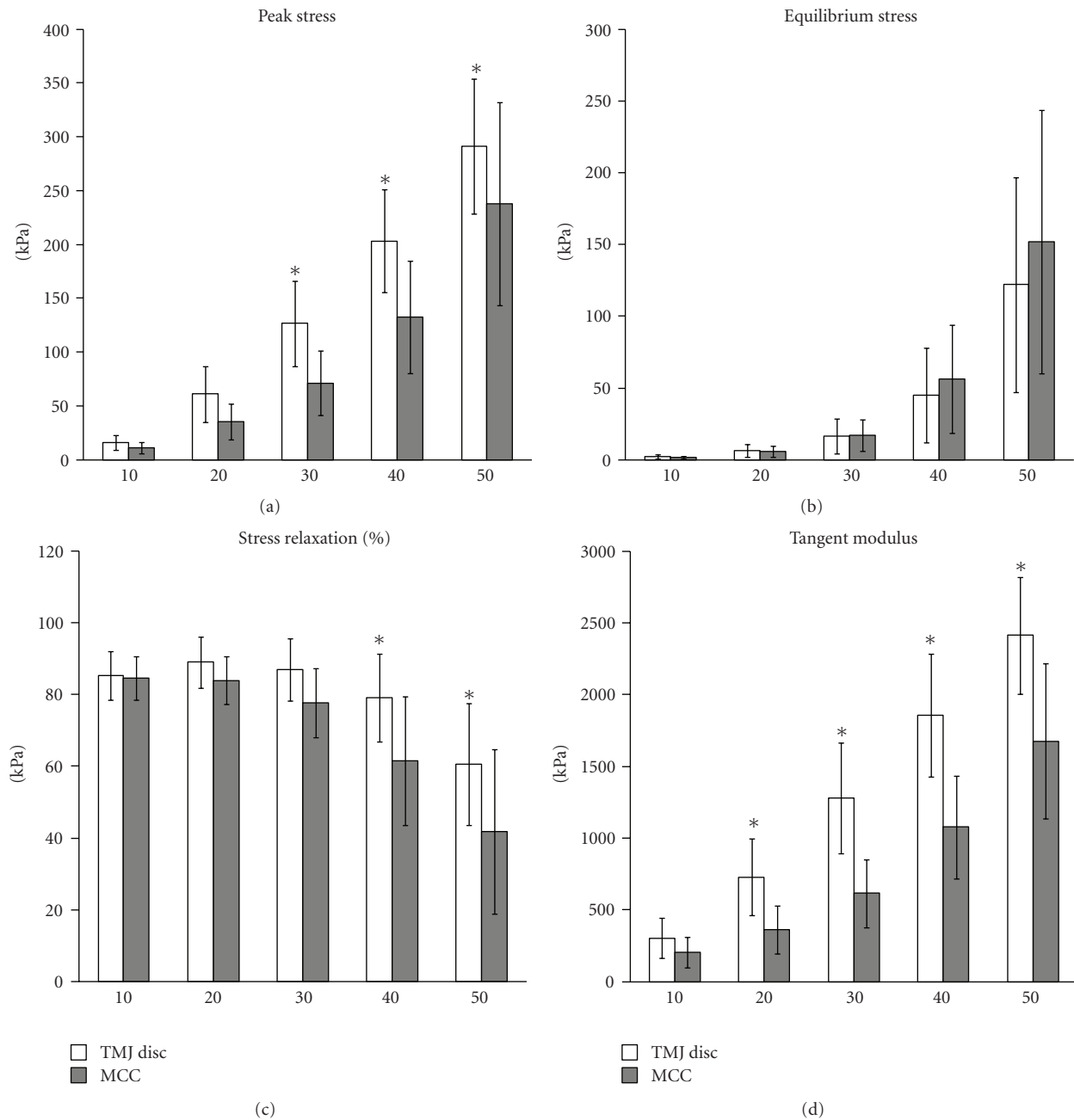
FIGURE 2: Simple compression analysis of the TMJ disc ($n = 8$ goats $\times$ $n = 3$ regions) and MCC ($n = 8$ goats $\times$ $n = 3$ regions) at 10%, 20%, 30%, 40%, and 50% strain. (a) Peak stress (b) Equilibrium stress (c) Percent stress relaxation (d). Tangent modulus. The symbol ($*$) indicates significance ($P < .05$) between the TMJ disc and MCC at each strain step. Error bars indicate S.D.

30% strain ($P < .05$). Conversely, with the equilibrium stress (Figure 2(b)), the differences between tissues were not significant. The equilibrium stress at 50% strain was significantly higher than all other strain steps ($P < .05$) for both the disc and the MCC at values of $122 \pm 75$ kPa and $152 \pm 92$ kPa, respectively (Table 1). The percent stress relaxation (Figure 2(c)) remained consistent between tissues at all strain levels until 40% strain when the MCC relaxed $62 \pm 18\%$, significantly less than the TMJ disc which relaxed $79 \pm 12\%$ ($P < .05$). The differences between strain levels for percent

relaxation were significant at high strain levels for both the disc and the MCC (Table 1). For instance, the disc relaxed $61 \pm 17\%$ at 50% strain, significantly less than $79 \pm 12\%$ at 40% strain. The MCC relaxed $62 \pm 18\%$ at 40% strain, significantly less than $78 \pm 10\%$ at 30% strain ($P < .05$). The TMJ disc showed a significantly higher tangent modulus than the MCC at all levels beyond 10% (Figure 2(d)). For example, at 20% strain the tangent modulus of the TMJ disc was $729 \pm 267$ kPa, significantly greater than the MCC which was $363 \pm 169$ kPa. There were also significant differences between

strain level for the tangent moduli of both the disc and MCC (Table 1). For instance, the tangent modulus for the disc significantly increases from $304 \pm 141$ kPa at 10% strain to $2413 \pm 406$ kPa at 50% strain ($P < .05$). The tangent modulus for the MCC significantly increases from $205 \pm 107$ kPa at 10% strain to $1677 \pm 538$ kPa at 50% strain ($P < .05$).

*3.2. Transversely Isotropic Biphasic Model.* It was determined that the transversely isotropic biphasic model provided a good fit for the stress response of the TMJ disc and MCC up to 30% strain. Since the relaxation profile for 40% and 50% strain changed, this data was not fitted to the model. The average stress response and curve fit for the TMJ disc and MCC at 10%, 20%, and 30% strain is shown in Figure 3. The results predicted by the transversely isotropic biphasic model are shown in Table 2. The model provided a better fit for the relaxation portion of the curve due to the fact that more data points were collected and utilized from the 30-minute relaxation period compared to the short ramping period. The results show an increase in $E_1$, $E_3$, and $\nu_{31}$ from 10% to 30% strain in both the TMJ disc and MCC. Conversely, there is a decrease in $k$ with increasing strain level in both tissues. The TMJ disc had a greater $E_1$ and $E_3$ than the MCC at all strain levels. For example, at 10% strain $E_1$ of the disc is 0.18 MPa, while that of the MCC is 0.14 MPa. Overall, the MCC exhibited a greater tissue permeability than the TMJ disc at all strain levels. For example, the permeability of the MCC at 10% strain was $5.48 \times 10^{-14}$ m$^4$/Ns, while the TMJ disc was $4.47 \times 10^{-14}$ m$^4$/Ns.

*3.3. Biochemical and Histological Analysis.* The results from the biochemical assessment also showed no statistically significant differences between the three regions in both the MCC and TMJ disc. Therefore, the regions were combined and results are presented by tissue type (Figures 4(a)–4(d)). The percent collagen content per dry weight of the disc was $45.7 \pm 19.6\%$ which was significantly higher than the MCC with a collagen content of $18.6 \pm 6.9\%$ ($P < .05$) (Figure 4(a)). The GAG content per dry weight of the disc was $2.1 \pm 1.2\%$ which was significantly lower than that of the MCC with a dry weight of $4.2 \pm 2.1\%$ ($P < .05$) (Figure 4(b)). The DNA content per dry weight of the disc was $0.1 \pm 0.05\%$ which was also significantly lower than the MCC with a DNA content of $0.3 \pm 0.1\%$ ($P < .05$) (Figure 4(c)). The percent water content of the TMJ disc was found to be $79 \pm 8\%$, which was significantly lower than that of the MCC with a water content of $84 \pm 7\%$ ($P < .05$) (Figure 4(d)).

The results from the histological assessment are shown in Figure 5. There is no conclusive evidence of change in collagen fiber organization, orientation, integrity, or packing between the mechanically tested to 50% strain and untested TMJ disc.

## 4. Discussion

The goal of this study was to compare the mechanical and biochemical properties of the goat TMJ disc to the MCC. The results indicated that the TMJ disc exhibits a significantly greater tangent modulus and peak stress than the MCC. There were strain level dependencies in peak stress, equilibrium stress, percent relaxation, tangent modulus, Young's moduli, Poisson's ratio, and tissue permeability for both tissue types. The transverse isotropic biphasic model provided a good fit for the stress-relaxation behavior of both the TMJ disc and MCC up to 30% strain. Due to the change in relaxation behavior at 40% and 50% strain, this data was not applied to the model. Coinciding with previous findings, the current assessment showed that the goat TMJ disc is stiffer than the MCC, albeit using different testing methods [27]. This study showed that unlike a regional analysis of the porcine disc by Allen and Athanasiou [28], the goat disc does not seem to exhibit regional variations in mechanical properties with this testing protocol. Conversely, the lack of significant differences in the middle regions of the goat MCC corresponds with previous findings using the porcine model by Singh and Detamore [29]. Significant differences between the mechanical properties of the tissues at different strain levels shed light on the function of these tissues *in vivo*, suggesting a change in tissue behavior at higher strains.

The biphasic theory derived by Mow et al. [18] can be used to describe the behavior of the fibrocartilagenous tissues of the TMJ under compression by assuming that the solid matrix may be linearly elastic and isotropic or anisotropic, and that interstitial fluid are intrinsically incompressible, or that compression is only possible due to fluid exudation. Viscous dissipation is assumed to be a result of interstitial fluid flow relative to the porous permeable solid matrix, and frictional drag is directly proportional to the relative velocity and it may be strain dependent. Biphasic approaches have been utilized which require confined compression chambers [30] or indentation testing for the TMJ disc [31, 32]. In another study, using biphasic indentation creep analysis, Kim et al. found that the intermediate zone of the porcine TMJ disc exhibits an aggregate modulus of $18.6 \pm 5.2$ kPa and a permeability of $22.8 \pm 9.8 \times 10^{-15}$ m$^4$/Ns [33]. In contrast, an additional study found that in confined compression, the average aggregate modulus of the intermediate, lateral, and medial regions of human TMJ disc is $69.75 \pm 11.47$ kPa and the permeability is $3.75 \pm 0.72 \times 10^{-15}$ m$^4$/Ns [34]. The values obtained using biphasic models do not deviate greatly from what was obtained for the axial Young's modulus of the goat TMJ disc (20 kPa) at 10% strain. However, the tissue permeability of the goat TMJ disc was found to be $4.47 \times 10^{-14}$ m$^4$/Ns at 10% strain, which is greater than the previously reported findings.

The group from Dr. Athanasiou also showed that using a viscoelastic model, and a high strain rate, the instantaneous modulus for the TMJ disc was found to be around 500 kPa [28]. Additionally, when Dr. Detamore's group investigated the porcine MCC using a high strain rate it, Singh and Detamore demonstrated that the average elastic modulus ranged from about 0.8 to 1.5 MPa [29]. While these values exceed what was observed in the goat TMJ, it is likely that these differences are largely attributed to differences in strain rate, along with species variation, testing protocols, and modeling.
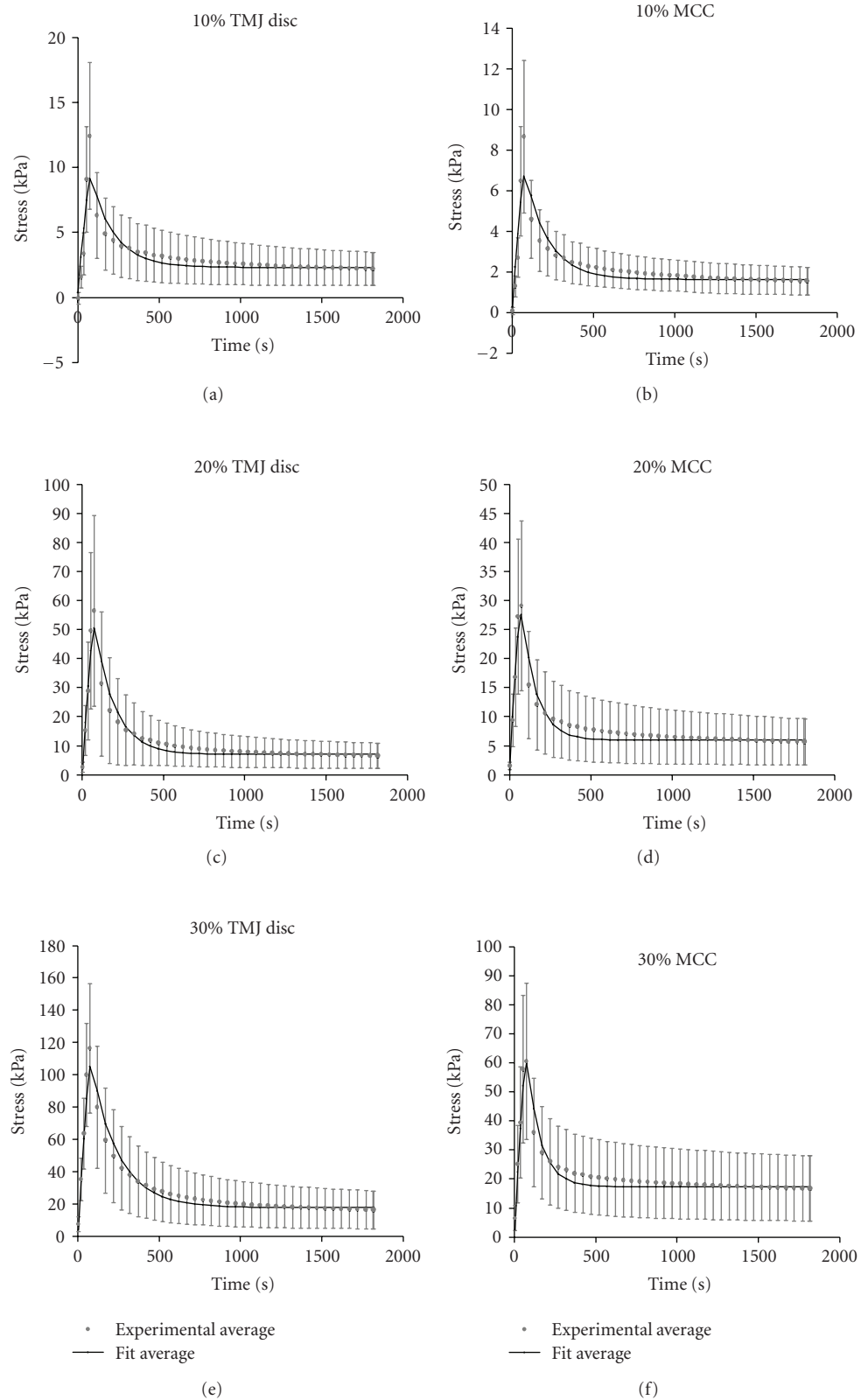
FIGURE 3: Average stress response of TMJ disc (a, c, and e) and MCC (b, d, and f) to 10%, 20%, and 30% strain and curve fit. The experimental average is the average stress response of all specimens with the error bars indicating standard deviation. The fit average was obtained by determining the best fit parameters for the average stress response.
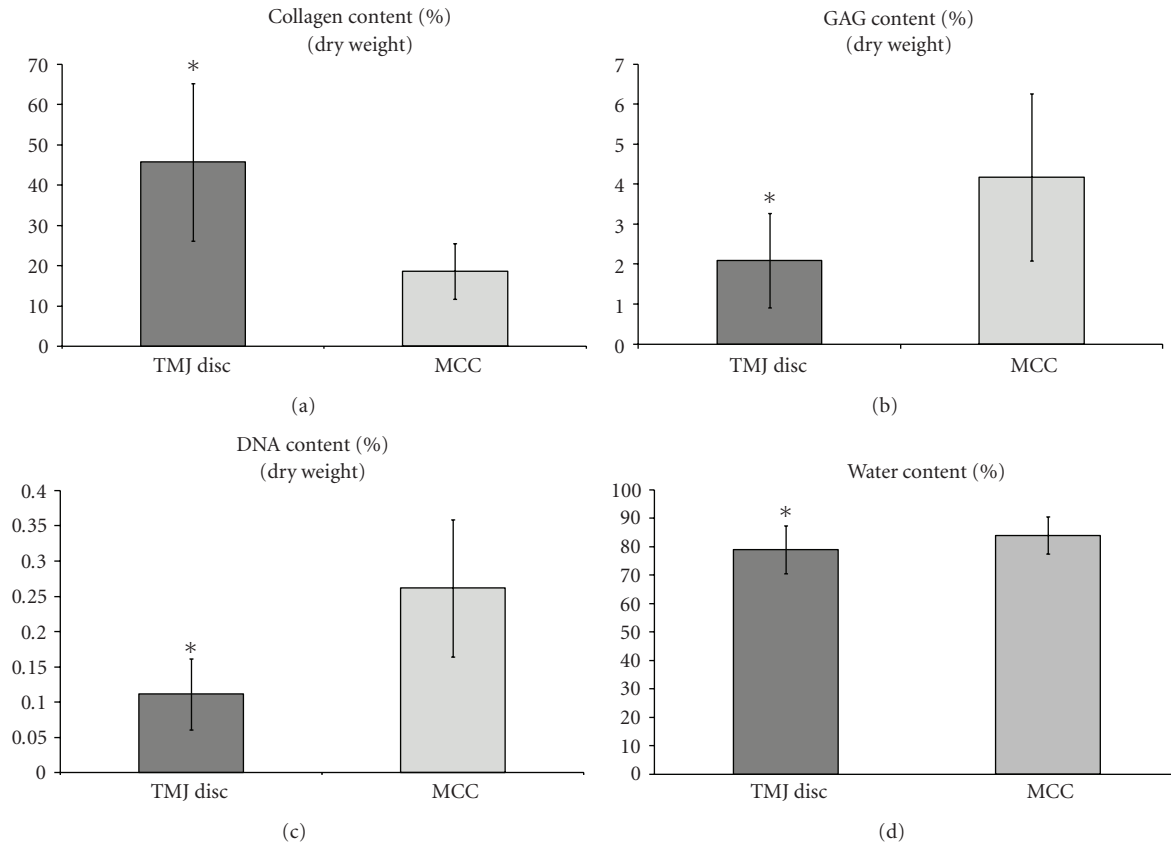
FIGURE 4: Biochemical analysis of the TMJ disc ($n = 8$ goats $\times$ $n = 3$ regions) and MCC ($n = 8$ goats $\times$ $n = 3$ regions). (a) Percent collagen content per dry weight. (b) Percent GAG content per dry weight. (c) Percent DNA content per dry weight. (d) Percent water content of the tissue. The symbol ($*$) indicates significance ($P < .05$) between the TMJ disc and MCC. Error bars indicate S.D.

The collagen content of the goat TMJ disc is less than that of the previously reported porcine ($68.2 \pm 14.5\%$) and human TMJ disc ($62.0 \pm 11.4$) [17, 34]. We did validate our collagen assay with porcine samples and obtained results comparable to literature [35]. Additionally, corresponding to our lack of significant differences in mechanical behavior between regions, there was no significant difference in biochemical content between regions. Further studies need to be performed to determine the remaining biochemical content of the goat disc and MCC. As for GAGs, the common concept of the role of GAGs is that they act to retain water molecules providing an added "cushion" under compression. However, this did not correspond to our findings where the TMJ disc, containing fewer GAGs than the MCC, had a higher tangent modulus. This seems to indicate that the collagen has an influence on mechanical support which outweighs that of the GAG, since GAG content might be too low to have a significant impact in force bearing.

A limitation of the transversely isotropic biphasic theory is that it assumes the solid matrix is homogenous and behaves linearly. It is known that the extracellular environment of both the disc and the MCC is inhomogeneous, and it is more likely that the solid part of the tissue exhibits viscoelastic behavior. Additionally, the theory assumes the application of low strain rates and lower applied strain,

which was pushed well pass 10% in this study. In the future, the use of alternate models, such as a finite element model, should be used to address the limitations of applying the transversely isotropic biphasic model to fibrocartilage when subject to high strain. Similarly, the application of a model that considers the compression-tension nonlinearity of tissues in unconfined compression stress relaxation, such as a fiber-reinforced model, may also provide for a more accurate depiction of the tissue behavior *in vivo*. The MCC, in general, provided for a better fit to the model than the disc. This difference was expected considering that the structure and composition of the disc and MCC are dissimilar. The TMJ disc consists of collagen arranged in tight bundles of anteroposteriorly oriented fibers in the zones that were tested [36]. In contrast, the MCC has a zonal organization of cartilage consisting of significantly less collagen and more GAG (Figures 4(a) and 4(b)). These structural differences affect the porosity of the solid matrix component and the ability to allow water flow. This is further supported by the finding that the water content of the disc is significantly lower than that of the MCC. (Figure 5(d)) These differences between the two tissues help explain why using a permeable, solid matrix model such as the transversely isotropic biphasic model is more appropriate for the MCC. A viscoelastic model may prove more appropriate for the TMJ disc, especially at
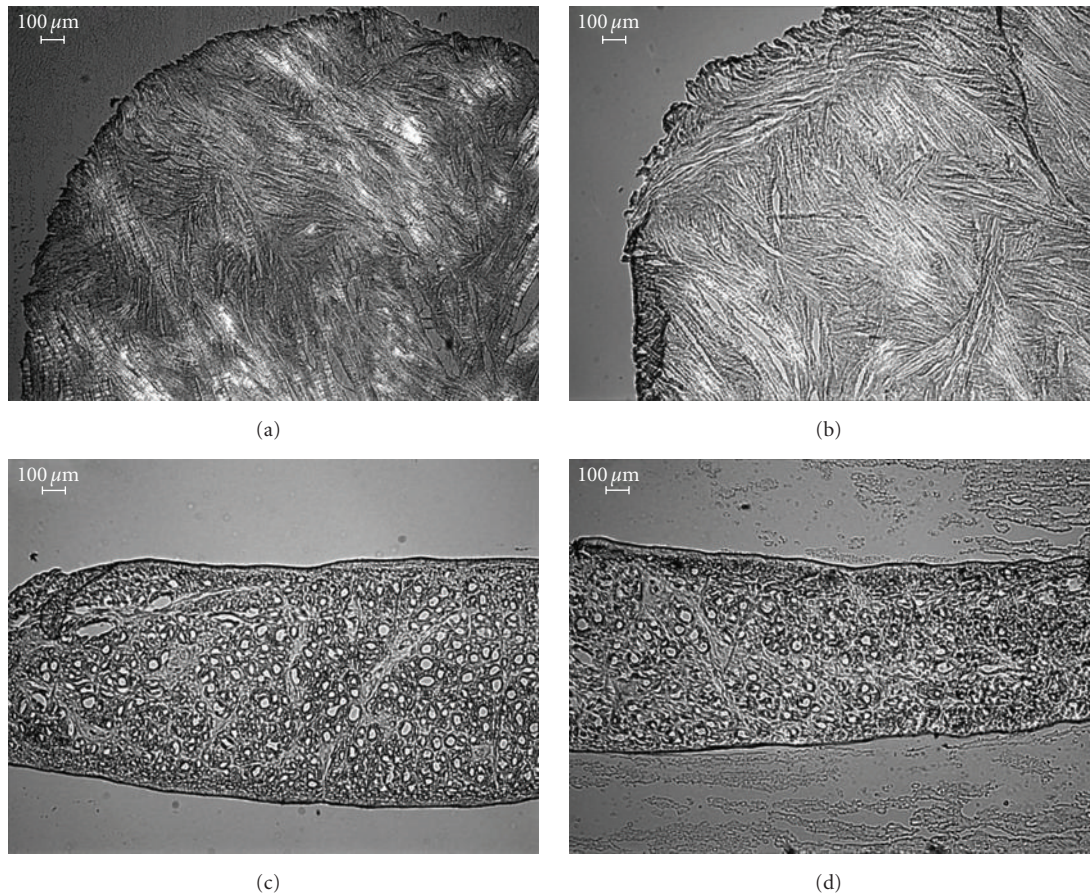
(a)

(b)

(c)

(d)

FIGURE 5: Polarized light image of the TMJ disc. (a) Transverse section of untested TMJ disc. (b) Transverse section of mechanically tested TMJ disc. (c) Axial section of untested TMJ disc. (d) Axial section of mechanically tested TMJ disc.

higher strain rates [28]. Another limitation might be the shorter relaxation time of 30 minutes. However, on average, in the last minute of the stress relaxation period, there was never a change of force greater than 0.01 N at all strain levels for both tissues. Lastly, this study did not quantify and characterize the various types of collagen and proteoglycans found in both the TMJ disc and MCC, which could further explain the differences in behavior.

Establishing the differences in composition and function of the disc and MCC is necessary for understanding the way these tissues interact *in vivo*. While both tissues are classified as fibrocartilagenous, this study elucidated important distinctions between the two-joint tissues. As the joint tissues become better characterized, the appropriate design criteria for tissue-engineered constructs can be established. The information from this study provides a necessary framework for the development of devices that alleviate the symptoms of TMDs.

## Acknowledgments

## References

[1] NIH, "TMJ disorders," 2010, http://www.nidcr.nih.gov/Oral-Health/Topics/TMJ/TMJDisorders.

[2] C. H. Wilkes, "Internal derangements of the temporomandibular joint. Pathological variations," *Archives of Otolaryngology—Head and Neck Surgery*, vol. 115, no. 4, pp. 469–477, 1989.

[3] C. Mejersjo and L. Hollender, "Radiography of the temporomandibular joint in female patients with TMJ pain or dysfunction. A seven year follow-up," *Acta Radiologica: Diagnosis*, vol. 25, no. 3, pp. 169–176, 1984.

[4] G. A. Zarb and G. E. Carlsson, "Temporomandibular disorders: osteoarthritis," *Journal of Orofacial Pain*, vol. 13, no. 4, pp. 295–306, 1999.

[5] W. B. Farrar and W. L. McCarty Jr., "The TMJ dilemma," *The Journal of the Alabama Dental Association*, vol. 63, no. 1, pp. 19–26, 1979.

[6] E. Tanaka and T. van Eijden, "Biomechanical behavior of the temporomandibular joint disc," *Critical Reviews in Oral Biology and Medicine*, vol. 14, no. 2, pp. 138–150, 2003.

[7] M. Singh and M. S. Detamore, "Stress relaxation behavior of mandibular condylar cartilage under high-strain compression," *Journal of Biomechanical Engineering*, vol. 131, no. 6, Article ID 061008, 2009.

[8] T. Hansson, T. Oberg, G. E. Carlsson, and S. Kopp, "Thickness of the soft tissue layers and the articular disk in the temporomandibular joint," *Acta Odontologica Scandinavica*, vol. 35, no. 2, pp. 77–83, 1977.

[9] T. Hansson and B. Nordström, "Thickness of the soft tissue layers and articular disk in temporomandibular joints with deviations in form," *Acta Odontologica Scandinavica*, vol. 35, no. 6, pp. 281–288, 1977.

[10] C. A. Bibb, A. G. Pullinger, and F. Baldioceda, "Serial variation in histological character of articular soft tissue in young human adult temporomandibular joint condyles," *Archives of Oral Biology*, vol. 38, no. 4, pp. 343–352, 1993.

[11] A. G. Pullinger, F. Baldioceda, and C. A. Bibb, "Relationship of TMJ articular soft tissue to underlying bone in young adult condyles," *Journal of Dental Research*, vol. 69, no. 8, pp. 1512–1518, 1990.

[12] C. P. Bosshardt-Luehrs and H. U. Luder, "Cartilage matrix production and chondrocyte enlargement as contributors to mandibular condylar growth in monkeys (*Macaca fascicularis*)," *American Journal of Orthodontics and Dentofacial Orthopedics*, vol. 100, no. 4, pp. 362–369, 1991.

[13] D. E. Anderson and K. A. Athanasiou, "Passaged goat costal chondrocytes provide a feasible cell source for temporomandibular joint tissue engineering," *Annals of Biomedical Engineering*, vol. 36, no. 12, pp. 1992–2001, 2008.

[14] D. E. Anderson and K. A. Athanasiou, "A comparison of primary and passaged chondrocytes for use in engineering the temporomandibular joint," *Archives of Oral Biology*, vol. 54, no. 2, pp. 138–145, 2009.

[15] M. Delatte, J. W. Von Den Hoff, R. E. M. van Rheden, and A. M. Kuijpers-Jagtman, "Primary and secondary cartilages of the neonatal rat: the femoral head and the mandibular condyle," *European Journal of Oral Sciences*, vol. 112, no. 2, pp. 156–162, 2004.

[16] A. Poikela, T. Kantomaa, P. Pirttiniemi, J. Tuukkanen, and K. Pietilä, "Unilateral masticatory function changes the proteoglycan content of mandibular condylar cartilage in rabbit," *Cells Tissues Organs*, vol. 167, no. 1, pp. 49–57, 2000.

[17] A. J. Almarza, A. C. Bean, L. S. Baggett, and K. A. Athanasiou, "Biochemical analysis of the porcine temporomandibular joint disc," *British Journal of Oral and Maxillofacial Surgery*, vol. 44, no. 2, pp. 124–128, 2006.

[18] V. C. Mow, S. C. Kuei, W. M. Lai, and C. G. Armstrong, "Biphasic creep and stress relaxation of articular cartilage in compression: theory and experiments," *Journal of Biomechanical Engineering*, vol. 102, no. 1, pp. 73–84, 1980.

[19] T. Shengyi and Y. Xu, "Biomechanical properties and collagen fiber orientation of TMJ discs in dogs: part 1. Gross anatomy and collagen fiber orientation of the discs," *Journal of Craniomandibular Disorders*, vol. 5, no. 1, pp. 28–34, 1991.

[20] M. Singh and M. S. Detamore, "Tensile properties of the mandibular condylar cartilage," *Journal of Biomechanical Engineering*, vol. 130, no. 1, Article ID 011009, 2008.

[21] B. Cohen, W. M. Lai, and V. C. Mow, "A transversely isotropic biphasic model for unconfined compression of growth plate and chondroepiphysis," *Journal of Biomechanical Engineering*, vol. 120, no. 4, pp. 491–496, 1998.

[22] K. D. Allen and K. A. Athanasiou, "A surface-regional and freeze-thaw characterization of the porcine temporomandibular

joint disc," *Annals of Biomedical Engineering*, vol. 33, no. 7, pp. 951–962, 2005.

[23] K. Sergerie, M. O. Lacoursière, M. Lévesque, and I. Villemure, "Mechanical properties of the porcine growth plate and its three zones from unconfined compression tests," *Journal of Biomechanics*, vol. 42, no. 4, pp. 510–516, 2009.

[24] B. M. Lempriere, "Poisson's ratio in orthotropic materials," *AIAA Journal*, vol. 6, no. 11, pp. 2226–2227, 1968.

[25] R. W. Farndale, C. A. Sayers, and A. J. Barrett, "A direct spectrophotometric microassay for sulfated glycosaminoglycans in cartilage cultures," *Connective Tissue Research*, vol. 9, no. 4, pp. 247–248, 1982.

[26] J. F. Woessner Jr., "The determination of hydroxyproline in tissue and protein samples containing small proportions of this imino acid," *Archives of Biochemistry and Biophysics*, vol. 93, no. 2, pp. 440–447, 1961.

[27] T. Kuboki, M. Shinoda, M. G. Orsini, and A. Yamashita, "Viscoelastic properties of the pig temporomandibular joint articular soft tissues of the condyle and disc," *Journal of Dental Research*, vol. 76, no. 11, pp. 1760–1769, 1997.

[28] K. D. Allen and K. A. Athanasiou, "Viscoelastic characterization of the porcine temporomandibular joint disc under unconfined compression," *Journal of Biomechanics*, vol. 39, no. 2, pp. 312–322, 2006.

[29] M. Singh and M. S. Detamore, "Stress relaxation behavior of mandibular condylar cartilage under high-strain compression," *Journal of Biomechanical Engineering*, vol. 131, no. 6, Article ID 061008, 2009.

[30] G. A. Ateshian, W. H. Warden, J. J. Kim, R. P. Grelsamer, and V. C. Mow, "Finite deformation biphasic material properties of bovine articular cartilage from confined compression experiments," *Journal of Biomechanics*, vol. 30, no. 11-12, pp. 1157–1164, 1997.

[31] A. F. Mak, W. M. Lai, and V. C. Mow, "Biphasic indentation of articular cartilage—I. Theoretical analysis," *Journal of Biomechanics*, vol. 20, no. 7, pp. 703–714, 1987.

[32] V. C. Mow, M. C. Gibbs, W. M. Lai, W. B. Zhu, and K. A. Athanasiou, "Biphasic indentation of articular cartilage—II. A numerical algorithm and an experimental study," *Journal of Biomechanics*, vol. 22, no. 8-9, pp. 853–861, 1989.

[33] K. W. Kim, M. E. Wong, J. F. Helfrick, J. B. Thomas, and K. A. Athansiou, "Biomechanical tissue characterization of the superior joint space of the porcine temporomandibular joint," *Annals of Biomedical Engineering*, vol. 31, no. 8, pp. 924–930, 2003.

[34] J. Kuo, L. Zhang, T. Bacro, and H. Yao, "The region-dependent biphasic viscoelastic properties of human temporomandibular joint discs under confined compression," *Journal of Biomechanics*, vol. 43, no. 7, pp. 1316–1321, 2010.

[35] K. N. Kalpakci et al., "An interspecies comparison of the temporomandibular joint disc," *Journal of Dental Research*, vol. 90, no. 2, pp. 193–198, 2011.

[36] A. M. Minarelli, M. Del Santo Jr., and E. A. Liberti, "The structure of the human temporomandibular joint disc: a scanning electron microscopy study," *Journal of Orofacial Pain*, vol. 11, no. 2, pp. 95–100, 1997.